Anionic and Neutral Complexes of Uracil and Water

O. Dolgounitcheva, V. G. Zakrzewski, and J. V. Ortiz*,†

Department of Chemistry, Kansas State University, Manhattan, Kansas 66506-3701

Received: June 14, 1999

Several isomeric structures of the uracil−water complex and its covalent-bound anion were calculated ab initio with second-order, many-body, perturbation theory and the 6-311++G** basis set. In all neutral complexes, water forms two hydrogen bonds with uracil. In each of the conventional anionic forms, a single, but stronger and shorter, hydrogen bond is found. All complexes are nonplanar, but ring-puckering is less pronounced in neutrals than in anions. Several isomers of the anionic uracil−water complex have positive adiabatic electron-detachment energies. The existence of multiple anionic isomers with vertical electron-detachment energies between 0.30 and 0.90 eV accounts for the broad photoelectron spectrum. The lowest unoccupied molecular orbital of the neutral complex at the geometry of the anionic complex provides a simple explanation for the structural and energetic consequences of electron attachment.

Introduction

Electron trapping by nucleotide bases has been studied extensively.[1] According to the conventional paradigm, an electron may be assigned to orbitals that consist of valence atomic functions or of lobes that are remote from the nuclear framework. In the former case, so-called valence-bound anions are expected to exhibit bond lengths and angles that contrast with those of the corresponding neutral species according to the interatomic phase relationships of an unoccupied molecular orbital of the neutral. In the latter case, so-called dipole-bound anions have small electron-detachment energies and minor geometrical differences with the corresponding neutral species, for the extra electron is bound loosely by the electrostatic field of the neutral.[2] Base anions formed in condensed media are commonly held to be valence-bound, with an electron assigned to a π orbital,[3,4] while anions of isolated bases in the gas phase are considered to be dipole-bound. The latter states are characterized in anion photoelectron experiments by a sharp, intense peak between 0 and 0.1 eV. Such features were recorded for gas-phase uracil (U), thymine, and cytosine.[5,6] Valence-bound anions of nucleotide bases have been observed in electron scattering experiments[7,8] and have been predicted on the basis of density functional theory (DFT) calculations.[9] Dipole-bound anions of U and other nucleotide bases have been predicted on the basis of calculations[10,11] with vertical electron-detachment energies (VEDEs) between 0.034 and 0.122 eV. The thermodynamic instability of the valence-bound U anion relative to the dipole-bound form was disclosed by recent ab initio calculations.[12]

Formation of anionic clusters of U and various numbers of water molecules was observed in crossed-beam, Rydberg electron-transfer (RET) experiments.[13] The (U·H₂O)⁻ species was characterized in anion photoelectron spectroscopy (PES) experiments by a broad feature with electron-detachment energies between 0.3 and 2.0 eV and a maximum near 0.9 eV.[14] No sharp, narrow feature between 0 and 0.1 eV was recorded. Such observations suggest that the (U·H₂O)⁻ complex has valence-bound character. Experimental confirmation has appeared recently[6] in a study where spectra of larger clusters were presented.

Three isomers of U−H₂O complexes and their anions were studied ab initio with second-order many-body perturbation theory (MBPT(2) or MP2) and the 6-31+G* basis set augmented with extra diffuse functions centered on a ghost atom at the positive end of a molecular dipole.[15] Optimization at the HF/6-31+G* level revealed planar structures for neutral and anionic complexes. In this study, only dipole-bound anions of U·H₂O were found and these appeared to be less stable with respect to electron detachment than dipole-bound U⁻.[10] A valence-bound U·(H₂O)⁻₃ cluster with a positive VEDE of 0.89 eV was found in similar studies.[16] However, this cluster was predicted to have a negative adiabatic electron affinity (AEA).

Three structures of U·H₂O complexes optimized with the B3LYP version of DFT and the 6-31++G** basis set have been reported recently.[17] Four neutral U-H₂O complexes were studied with many-body perturbation theory and a double-ζ basis set augmented with so-called interaction-optimized polarization functions.[18] Basis set superposition errors were considered as well.

In this work, electron affinities of valence-bound, U−H₂O complexes and electron-detachment energies of U−H₂O anions are studied with electron propagator theory[19] and many-body perturbation theory.[20] These calculations attempt to describe the species that are observed in the anion PES and RET experiments.

Methods

All calculations were performed with GAUSSIAN-98.[21]

Preliminary closed-shell Hartree−Fock (RHF) and unrestricted Hartree−Fock (UHF) geometry optimizations with C_1 symmetry were done on conventional U−H₂O complexes (A, B, C, and D), tautomeric U−H₂O complexes (A′, C′, and D′), and their respective ²A radical anions with the 6-31G* basis set.[22] Seven neutral and seven anionic minima were found for hydrogen-bonded nonplanar complexes of U and H₂O. These structures were further optimized at the MBPT(2) level for singlets or at the UHF-reference MBPT(2) level, or UMBPT-(2), for doublets with 6-311G** and 6-311++G** basis sets.[23] Spin-projected corrections to unrestricted second-order energies (PUMP2) were obtained for anionic structures.[24] Almost no spin contamination was produced in the UMBPT(2) calculations on

† E-mail: ortiz@ksu.edu.

Complexes of Uracil and Water

J. Phys. Chem. A, Vol. 103, No. 39, 1999 **7913**

TABLE 1: Dihedral Angles (deg)

	A	A⁻	B	B⁻	C	C⁻	D	D⁻	A′	A′⁻	C′	C′⁻	D′	D′⁻
$N_1C_1C_2C_3$	3.0	20.9	3.0	20.7	2.8	22.6	2.8	22.9	0	15.8	0	21.9	0.2	20.9
$H_1C_1N_1H_4$	7.6	38.0	8.1	38.6	6.7	33.3	7.9	36.4	0.5	44.4				
$H_1C_1N_1C_4$	3.5	10.2	3.6	10.9	3.0	10.7	3.5	10.3	0.5	11.3	0.3	8.7	1.8	13.8
$C_1N_1C_4N_2$	7.8	12.2	8.1	12.1	7.1	8.8	7.7	11.3	1.0	20.3	0.3	2.2	2.5	18.2
$C_1N_1C_4O_1$	5.9	11.9	6.2	12.0	5.3	9.4	5.8	11.4	1.0	17.9	0	1.5	2.2	16.3
CO···HO	4.9	13.8	3.0	26.6	1.6	22.8	5.6	27.0	8.3	2.9	6.6	5.5	10.8	7.0

TABLE 2: Hydrogen Bond Parameters (Å)

	A	A⁻	B	B⁻	C	C⁻	D	D⁻
=O···HOH	1.990	1.739	1.946	1.773	2.002	1.734	2.023	1.797
NH···OH₂	1.959	2.801			1.926	2.464	1.977	2.851
CH···OH₂			2.374	3.060				
OH	0.969	0.986	0.969	0.983	0.970	0.985	0.968	0.979
OH′	0.960	0.959	0.959	0.960	0.960	0.959	0.959	0.959

	A′	A′⁻	C′	C′⁻	D′	D′⁻
OH···OH₂	1.749	2.053	1.717	1.960	1.710	1.914
N···HOH	2.030	1.728	2.032	1.713	2.012	1.729
OH	0.973	1.001	0.973	1.003	0.975	1.002
OH′	0.960	0.960	0.960	0.960	0.960	0.960

the anions: $\langle s^2 \rangle$ values did not exceed 0.80 before projection and 0.751 after projection of quartet contaminants. Single-point calculations on optimized structures were performed with the 6-311++G(2df,2p) basis set.[25] AEAs were calculated as differences of anion PUMP2 and neutral MBPT(2) total energies at equilibrium geometries. VEDEs were calculated as the differences of anion PUMP2 energies and MBPT(2) energies of neutrals at optimized anion geometries and as vertical electron affinities of neutrals in the outer valence Green's function (OVGF) approximation[26] with the 6-311++G** basis set. Isotropic Fermi contact couplings (IFCCs) were calculated for doublets at the UMBPT(2) level with both basis sets.

All structures and orbitals were graphed with MOLDEN.[27]

Results and Discussion

A complete list of bond lengths and angles optimized at different levels is given in Tables S1−S7 of the Supporting Information. Structural data pertaining to ring puckering and hydrogen bond lengths are given in Tables 1 and 2. Total energies obtained with the 6-311++G** and 6-311++G-(2df,2p) basis sets are presented in Tables 3 and 4, respectively. Isomerization energies inferred from these data are summarized in Table 5. Table 6 contains hydrogen-bond energies. Table 7 presents VEDEs of anions and AEAs of neutral complexes. IFCCs are shown in Table 8. Table 9 contains zero-point corrections to total energies obtained at the SCF/6-31G* level. The atomic numbering scheme is presented by Figure 1. Figures 2−8 give front and side views of all complexes. Molecular orbital plots are displayed in Figure 9.

Neutral U−H₂O Complexes. Four minima pertaining to conventional U−H₂O hydrogen-bonded complexes and three minima corresponding to tautomeric structures were obtained in preliminary geometry optimizations at the HF/6-31G* level. All complexes are strongly bound and form pseudocyclic, hydrogen-bonded structures. Tautomeric structures are related to conventional structures by rearrangement of hydrogen bonds in six-member rings. Structures were reoptimized with MBPT-(2) and the 6-311++G** basis set. The relative stability of the complexes decreases in the following order: C > A > D > B > C′ > A′ > D′.

Structures. All neutral complexes exhibit nonplanar U rings and hydrogen-bonded rings. The water molecule is a proton donor and a proton acceptor; these two hydrogen bonds form

TABLE 3: 6-311++G Total Energies (au)**

procedure		geometry		energy
U	MBPT(2)	U	MBPT(2)	−413.849 59
²A′ U⁻	UMBPT(2)	²A′ U⁻	UMBPT(2)	−413.834 86
	PUMP2		UMBPT(2)	−413.834 89
² A U⁻	UMBPT(2)	²A U⁻	UMBPT(2)	−413.834 28
	PUMP2		UMBPT(2)	−413.838 16
U(A′)	MBPT(2)	U(A′)	MBPT(2)	−413.831 57
U(C′)	MBPT(2)	U(C′)	MBPT(2)	−413.833 86
U(D′)	MBPT(2)	U(D′)	MBPT(2)	−413.821 09
H₂O	MBPT(2)	H₂O	MBPT(2)	−76.274 92
A	MBPT(2)	A	MBPT(2)	−490.139 94
A⁻	UMBPT(2)	A⁻	UMBPT(2)	−490.131 86
A⁻	PUMP2	A⁻	UMBPT(2)	−490.136 38
A	MBPT(2)	A⁻	UMBPT(2)	−490.105 84
B	MBPT(2)	B	MBPT(2)	−490.136 97
B⁻	UMBPT(2)	B⁻	UMBPT(2)	−490.132 96
B⁻	PUMP2	B⁻	UMBPT(2)	−490.137 30
B	MBPT(2)	B⁻	UMBPT(2)	−490.104 19
C	MBPT(2)	C	MBPT(2)	−490.142 51
C⁻	UMBPT(2)	C⁻	UMBPT(2)	−490.129 89
C⁻	PUMP2	C⁻	UMBPT(2)	−490.133 88
C	MBPT(2)	C⁻	UMBPT(2)	−490.110 61
D	MBPT(2)	D	MBPT(2)	−490.139 33
D⁻	UMBPT(2)	D⁻	UMBPT(2)	−490.128 31
D⁻	PUMP2	D⁻	UMBPT(2)	−490.132 23
D	MBPT(2)	D⁻	UMBPT(2)	−490.105 65
A′	MBPT(2)	A′	MBPT(2)	−490.126 93
A′⁻	UMBPT(2)	A⁻	UMBPT(2)	−490.117 95
A⁻	PUMP2	A⁻	UMBPT(2)	−490.123 70
A′	MBPT(2)	A⁻	UMBPT(2)	−490.095 98
C′	MBPT(2)	C′	MBPT(2)	−490.129 01
C⁻	UMBPT(2)	C⁻	UMBPT(2)	−490.108 32
C⁻	PUMP2	C⁻	UMBPT(2)	−490.114 50
C′	MBPT(2)	C⁻	UMBPT(2)	−490.103 31
D′	MBPT(2)	D′	MBPT(2)	−490.118 84
D⁻	UMBPT(2)	D⁻	UMBPT(2)	−490.096 19
D⁻	PUMP2	D⁻	UMBPT(2)	−490.099 67
D′	MBPT(2)	D⁻	UMBPT(2)	−490.088 59

TABLE 4: 6-311++G(2df,2p) Total Energies[a] (au)

procedure		energy
A	MBPT(2)	−490.403 50
A⁻	UMBPT(2)	−490.398 58
A⁻	PUMP2	−490.403 26
B	MBPT2	−490.400 45
B⁻	UMBPT(2)	−490.399 47
B⁻	PUMP2	−490.403 99
C	MBPT2	−490.405 98
C⁻	UMBPT(2)	−490.396 80
C⁻	PUMP2	−490.400 99
D	MBPT2	−490.402 76
D⁻	UMBPT(2)	−490.395 02
D⁻	PUMP2	−490.399 13
A′	MBPT(2)	−490.390 92
A′⁻	UMBPT(2)	−490.384 51
A′⁻	PUMP2	−490.390 33

[a] The same geometries as in Table 3.

six-member rings. Deviations from planarity are as large as 8°. This nonplanarity was obtained only with optimizations at the MBPT(2) level. Structures optimized at the SCF level are almost planar, except for the water fragment.

TABLE 5: Isomerization Energies (kcal/mol)

| U·H₂O | ΔMBPT(2) | | U⁻·H₂O | ΔUMBPT(2) | | ΔPUMP2 | |
	6-311++G**	6-311++G(2df,2p)		6-311++G**	6-311++G(2df,2p)	6-311++G**	6-311++G(2df,2p)
C	0	0	C⁻	1.93	1.67	2.15	1.88
A	1.61	1.56	A⁻	0.69	0.56	0.58	0.45
D	2.00	2.02	D⁻	2.92	2.79	3.18	3.05
B	3.48	3.47	B⁻	0	0	0	0
C′	8.47		C′⁻	15.46		14.31	
A′	9.78	9.45	A′⁻	9.42	9.39	8.54	8.57
D′	14.85		D′⁻	23.07		23.61	

TABLE 6: Hydrogen Bond Energies (ΔE^a) (kcal/mol)

	A	B	C	D	A′	C′	D′
MBPT(2)	9.7	7.8	11.3	9.3	12.8	12.7	14.3
MBPT(2)+ZPE	7.4	5.8	8.9	7.1	10.3	10.1	11.6
MBPT(2) + BSCC	7.7	6.2	9.2	7.3	10.7	10.6	12.2

	A⁻	B⁻	C⁻	D⁻	A′⁻	C′⁻	D′⁻
UMBPT(2)	14.2	14.9	13.0	12.0			
UMBPT(2) + ZPE	11.8	12.6	10.6	9.8			
UMBPT(2) + BSCC	12.4	13.2	11.3	10.2	14.9	15.1	16.0
PUMP2	14.6	15.2	13.0	12.0			
PUMP2 + ZPE	12.2	12.9	10.6	9.8			
PUMP2 + BSSC	12.7	13.4	11.4	10.3	15.2	14.3	16.0

^{a} $\Delta E = E_{\text{total}}(\text{U}) + E_{\text{total}}(\text{H}_2\text{O}) - E_{\text{total}}(\text{complex})$.

The U fragment's bond lengths and bond angles do not differ much from optimized values of free U.[12] Hydrogen bonds formed between an amino hydrogen and water are shorter than the corresponding −C=O···HOH bond. The difference is about 0.03−0.05 Å in complexes A and D and about 0.08 Å in complex C. Our MBPT(2) results differ from optimized values obtained for A, C, and D in ref 17 with B3LYP/6-31++G**. While the DFT distances for the NH···OH₂ hydrogen bond are essentially the same as ours, the DFT −C=O···HOH hydrogen bond lengths are 0.05−0.07 Å shorter. For the tautomeric complexes A′−D′, the OH···OH₂ hydrogen bonds are 0.21−0.27 Å smaller than the corresponding NH···OH₂ bonds in conventional complexes. N···HOH hydrogen bonds in A′ and C′ are slightly longer than their =O··HOH counterparts in A and C.

Energies. Hydrogen bond energies inferred from total energies are reported in Table 6. (Total energies of H₂O, U, and U tautomers whose structures resemble those of the U fragments in the A′, C′, and D′ complexes are reported in Table 3; the ²A′ U⁻ entries refer to a planar, dipole-bound form.[12]) All complexes are strongly bound. Hydrogen bond energies in Table 6 are between 7.8 and 11.3 kcal/mol for conventional complexes and are between 12.7 and 14.3 kcal/mol for tautomeric complexes. Basis set counterpoise corrections (BSCC)[28] with the present methods do not exceed 2 kcal/mol. Zero-point energy (ZPE) corrections have a comparable lowering effect on the hydrogen bond energies. A−B and C−D pairs of complexes are positional isomers with one common hydrogen bond. Isomerization barriers are likely to be high enough to imply that all four isomers may be present in the gas phase or under conditions of matrix isolation. Whether the tautomeric complexes can be observed under the same conditions is doubtful, as these are 8−15 kcal/mol higher in energy than the conventional complexes (see Table 5). However, it is noteworthy that for the A/A′ and C/C′ pairs, 8 kcal/mol energy differences between conventional and tautomeric complexes are less than those between isolated U and its tautomeric forms U(A′), U(C′), and U(D′), 11, 10, and 18 kcal/mol, respectively (see Table 3). A recent study employing smaller basis sets[29] found isomerization energies between 11 and 13 kcal/mol for several tautomers.

These findings imply that water complexation reduces the relative instability of the tautomeric forms.

Anions. *Structures.* Comparison of optimized anionic and neutral complex structures presented in Figures 2−8 reveals that electron attachment leads to major structural changes. Ring puckering is significant (Table 1) and rings formed by hydrogen bonds are opened. In all conventional anionic complexes, the NH···OH₂ bonds are broken and the remaining −C=O···HOH bonds, while remaining nonlinear, are much shorter than they are in the neutrals. Bond lengths and bond angles of the ring are very close to the values obtained for ²A U⁻ and optimized at the same level.[12]

The basis set dependences of MBPT(2) geometries are reflected in Tables S1−S7 of the Supporting Information. In both neutral and anionic complexes, parameters of the U ring are approximately unchanged when the 6-311G** basis set is augmented with diffuse functions on all atoms. Hydrogen-bond parameters change significantly for anions. While the =O··· HOH bond lengths change by ±0.032 Å, the −H···OH₂ bonds are always longer in anionic complexes optimized with the largest basis set. Differences in optimized values vary from ∼0.20 Å in C⁻ to ∼0.56 Å in A⁻.

Energies. Anionic complexes are stable with respect to dissociation to U⁻ and water. The stability of the conventional anions decreases in the following order: B⁻ ≈ A → C⁻ > D⁻. Hydrogen bonding becomes stronger upon anion formation, and for complex B⁻, the bond energy is approximately doubled. A single hydrogen bond in the anionic complexes is generally stronger than two ring-forming hydrogen bonds in the neutral complexes.

VEDEs and AEAs. AEAs of U·H₂O complexes were calculated as differences of MBPT(2) total energies of neutrals and PUMP2 total energies of anions. (This approximation's accuracy for U⁻ was confirmed recently by coupled-cluster results at the CCSD(T) level.[12]) ΔUMBPT(2) values were calculated as well. Complex B has a small, positive AEA at the PUMP2 level. A 10-fold increase of this value is obtained with the 6-311++G-(2df,2p) basis. AEAs of other complexes are negative at this level. ZPE corrections to AEA values were determined with RHF/6-31G* and UHF/6-31G* calculations and are reported in Table 9. For the A/A⁻ pair, RHF and UHF geometries were reoptimized and ZPEs were calculated with the 6-311++G** basis. The resulting ZPE correction, 0.123 eV, coincided with the 6-31G* value. Therefore, for all other tautomers, ZPEs at the HF/6-31G* level were incorporated into AEAs. With this approach, two other structures, A and A′, acquire positive AEAs. C′ and D′ have large, negative AEAs and are unlikely to form gas-phase anions. Single-point calculations repeated with the 6-311++G(2df,2p) basis produce positive AEAs for A, B, D, and A′ after the ZPE correction is added.

All anions display positive VEDEs at the PUMP2 and UMBPT(2) levels, but C′⁻ and D′⁻ have negative VEDEs in the OVGF approximation. The largest VEDEs obtain for B⁻. The A⁻, D⁻, and C⁻ structures provide close but steadily

Complexes of Uracil and Water

J. Phys. Chem. A, Vol. 103, No. 39, 1999 **7915**

TABLE 7: AEAs and VEDEs (eV)

complex	method	AEA 1[a]	AEA 2[a]	AEA + ZPE 2[a]	anion	method	VEDE 1[a]
A	PUMP2	−0.097	−0.006	0.117	A⁻	PUMP2	0.83
	UMBPT(2)	−0.220	−0.134	−0.011		UMBPT(2)	0.71
						OVGF	0.44
B	PUMP2	0.009	0.096	0.214	B⁻	PUMP2	0.90
	UMBPT(2)	−0.109	−0.027	0.091		UMBPT(2)	0.78
						OVGF	0.54
C	PUMP2	−0.235	−0.136	−0.007	C⁻	PUMP2	0.63
	UMBPT(2)	−0.343	−0.250	−0.121		UMBPT(2)	0.52
						OVGF	0.25
D	PUMP2	−0.193	−0.099	0.032	D-	PUMP2	0.72
	UMBPT(2)	−0.300	−0.210	−0.080		UMBPT(2)	0.62
						OVGF	0.28
A′	PUMP2	−0.088	−0.016	0.116	A′⁻	PUMP2	0.75
	UMBPT(2)	−0.244	−0.174	−0.042		UMBPT(2)	0.60
						OVGF	0.36
C′	PUMP2	−0.39			C′⁻	PUMP2	0.30
	UMBPT(2)	−0.560				UMBPT(2)	0.14
						OVGF-	−0.34
D′	PUMP2	−0.52			D′⁻	PUMP2	0.30
	UMBPT(2)	−0.616				UMBPT(2)	0.21
						OVGF	−0.26

[a] Basis sets: 1 = 6-311++G**; 2 = 6-311++G(2df,2p).

TABLE 8: Isotropic Fermi Contact Couplings (gauss)

basis	anion	A⁻	B⁻	C⁻	D⁻	A′⁻	C′⁻	D′⁻
6-311++G**	C_1	82.0	83.3	81.0	80.0	81.0	67.8	79.0
6-311++G(2df,2p)		83.2	84.4	82.2	83.0	81.1		
6-311++G**	H_1	−14.6	−14.5	−14.6	−12.9	−14.4	−24.8	−3.5
6-311++G(2df,2p)		−14.2	−14.2	−14.2	−12.6	−14.0		

TABLE 9: Zero-Point Energy Corrections (au)

neutral	correction	anion	correction
A	0.121 26	A⁻	0.116 73
A[a]	0.119 67	A⁻[a]	0.115 13
B	0.120 79	B⁻	0.116 46
C	0.121 43	C⁻	0.116 69
D	0.121 16	D⁻	0.116 35
A′	0.121 43	A′⁻	0.116 56
C′	0.121 50	C′⁻	0.116 06
D′	0.121 21	D′⁻	0.117 06
U	0.094 62	U⁻	0.089 88
H_2O	0.022 98		

[a] Calculated in 6-311++G** basis set.
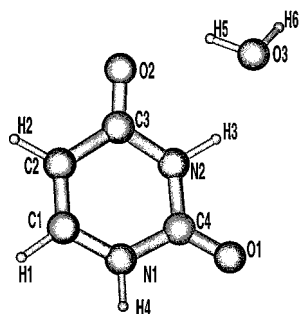
Figure 1. Atomic numbering scheme.

Figure 2. Complex A and complex A⁻.

decreasing VEDEs. All of the positive VEDEs of Table 7 are compatible with the broad feature found in anion PES experiments.[6,14] The VEDE of the most stable anion, B⁻, coincides with the maximum seen near 0.8−0.9 eV. The presence of several isomers may be responsible for the shape of this broad band.

VEDEs assessed at the UMBPT(2) level of theory are only 0.1 eV smaller than the PUMP2 values. The OVGF VEDEs are systematically smaller than either PUMP2 or UMBPT(2)

VEDEs. This trend is probably produced by incomplete treatment of orbital relaxation in this approximation. All three renormalization procedures[30,31] produce results that are within 0.07 eV of the recommended values given in Table 7.

Larger basis sets and more complete correlation methods are likely to produce larger VEDEs and AEAs. Extra polarization functions present in the 6-311++G(2df,2p) basis produce a positive AEA for D. Additional basis set improvements could change the sign of the C AEA.

IFCCs. As was the case with the ²A U radical anion,[12] the highest IFCC values occur at the most pyramidalized atom, C_1. The absolute values obtained at H_1, 12.6−14.2 G, are very close to the experimental result observed by Sevilla for U in solution,
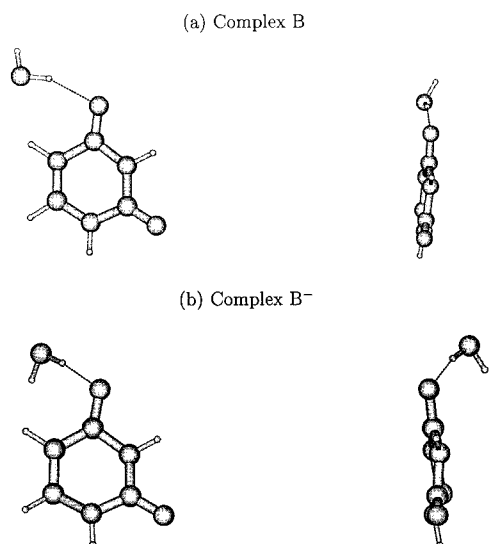
Figure 3. Complex B and complex B⁻.
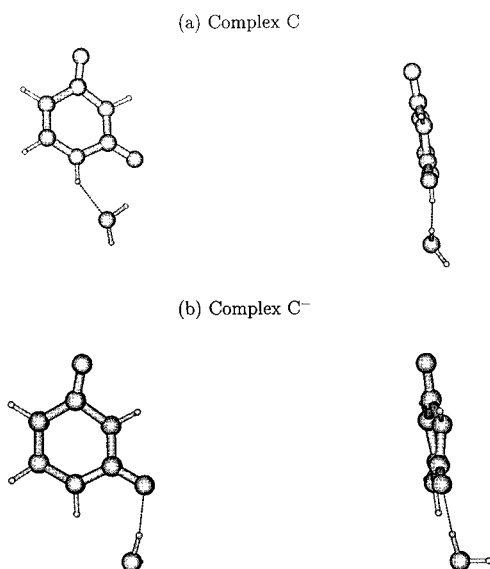
Figure 4. Complex C and complex C⁻.
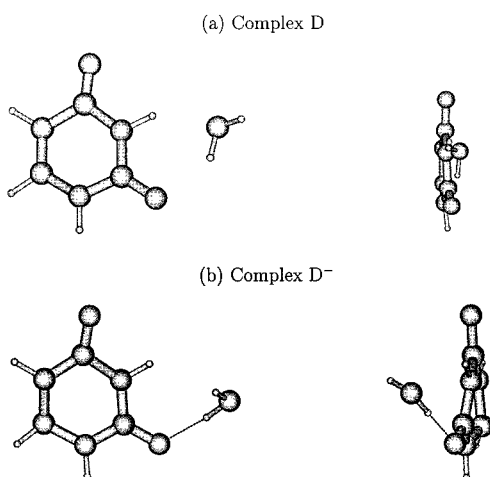
Figure 5. Complex D and complex D⁻.

13 G.[32] Inclusion of additional polarization functions into the valence part of the basis set changes the IFCCs slightly.

Molecular Orbitals. The highest, singly-occupied molecular orbitals (SOMOs) of the four conventional anions and the lowest
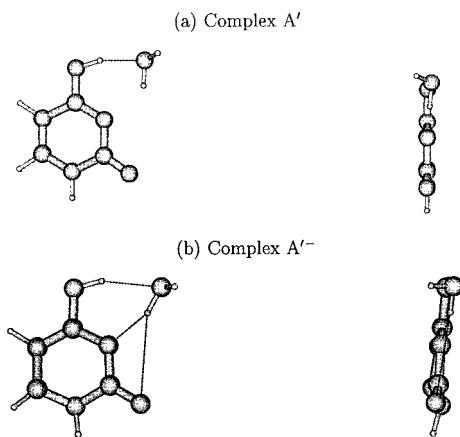
Figure 6. Complex A′ and complex A′⁻.
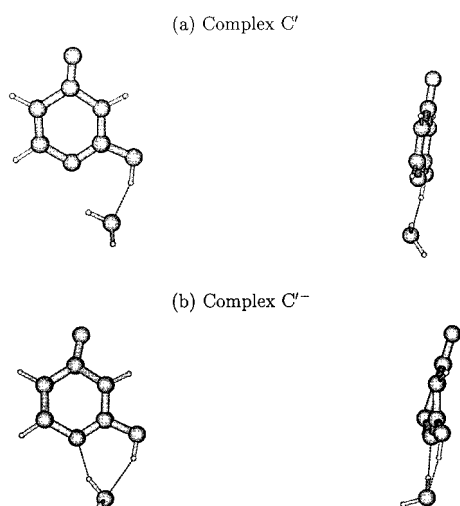
Figure 7. Complex C′ and complex C′⁻.
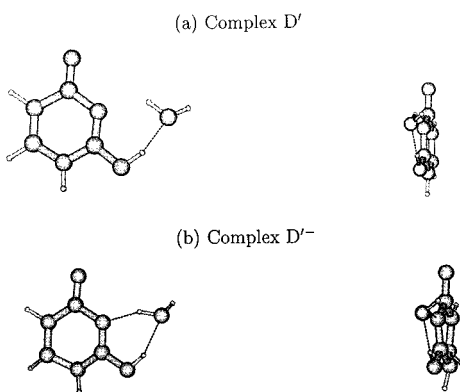
Figure 8. Complex D′ and complex D′⁻.

unoccupied molecular orbitals (LUMOs) of the neutrals at the geometries of these anions are very much alike. Therefore, only the SOMO of A⁻ and the LUMO of A are depicted in parts a and b of Figure 9. Ordinary valence basis functions are the chief contributors to these orbitals.

Large amplitudes near the C_2, C_3, and O_2 positions imply that electronic charge accumulates in this region upon electron attachment. Π-antibonding relationships in the ring are alleviated by puckering and pyramidalization at the C_1 nucleus. Whereas the most stable isomer is C for the neutral complex, the lowest isomer of the anion becomes B⁻, where the water molecule engages the O_2 center in a hydrogen bond. The relative stability of the A⁻ isomer also is enhanced. Hydrogen bonding in the A

Complexes of Uracil and Water

J. Phys. Chem. A, Vol. 103, No. 39, 1999 **7917**

(a)   (b)

(c)   (d)
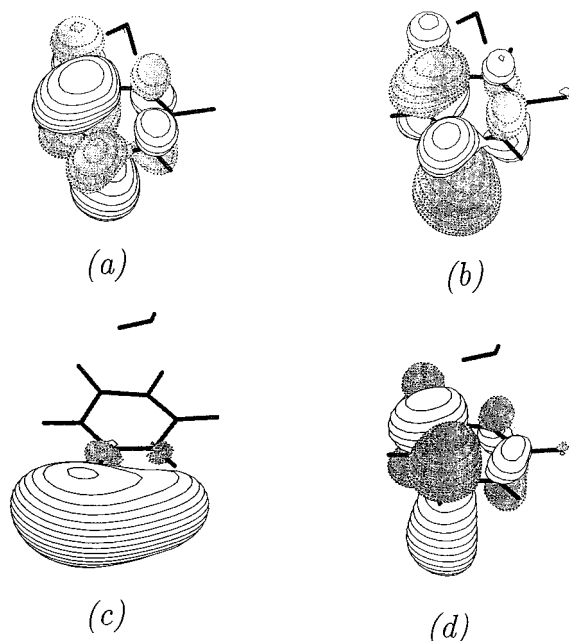
Figure 9. (a) Singly-occupied molecular orbital (SOMO) of complex A^-. (b) Lowest unoccupied molecular orbital (LUMO) of complex A at the geometry of A^-. (c) LUMO of complex A. (d) A higher unoccupied molecular orbital of complex A.

and B forms enhances the stability of the corresponding valence-bound anions.

For neutral complexes at their optimum geometries, the LUMO consists chiefly of diffuse functions. The resulting plot, shown in Figure 9c, resembles the diffuse lobes that characterize dipole-bound anions, for the largest amplitudes are distant from the nuclear framework. An unoccupied orbital, depicted in Figure 9d, bears close resemblance to the anion SOMO and to the neutral LUMO obtained at the anion geometry. This orbital, whose energy is 1.3 eV higher, has a large p contribution at the C_1 position that is in an antibonding relationship with neighboring atoms. U ring puckering diminishes this destabilizing relationship.

Conclusions

Several neutral and anionic complexes of uracil and water were found in MBPT(2) calculations. Anion VEDEs of all anions lie between 0.3 and 0.9 eV. At least four structures have positive AEAs. The VEDE of the most stable anion structure is 0.9 eV and coincides well with the experimentally observed maximum in a broad spectral feature. The breadth of this feature is due to the presence of several isomers of the anionic uracil-water complex. The uracil ring in all complexes is nonplanar. Attachment of an electron to a valence unoccupied molecular orbital of the neutral complex leads to ring puckering and enhanced stability for hydrogen bonds in the A and B complexes.

Supporting Information Available: Tables S1−S7 listing bond lengths and optimized angles. This material is available free of charge via the Internet at http://pubs.acs.org.

References and Notes

(1) Colson, A. O.; Sevilla, M. D. *Int. J. Radiat. Biol.* **1995**, *67*, 627 and references therein.

(2) This model predicts that electron-detachment energies of dipole-bound anions increase with increasing dipole moments. In principle, a dipole-bound anion could have a large electron-detachment energy.

(3) Steenken, S. *Chem. Rev.* **1989**, *89*, 503.

(4) Sevilla, M. D.; Besler, B. B.; Colson, A. O. *J. Phys. Chem.* **1994**, *98*, 2215.

(5) Hendricks, J. H.; Lyapustina, S. A.; de Clercq, H. L.; Snodgrass, J. T.; Bowen, K. H. *J. Chem. Phys.* **1996**, *104*, 7788.

(6) Schiedt, J.; Weinkauf, R.; Neumark, D. M.; Schlag, E. W. *Chem. Phys.* **1998**, *239*, 511.

(7) Aflatooni, K.; Gallup, G. A.; Burrow, P. D. *J. Phys. Chem. A* **1998**, *102*, 6205.

(8) Huels, M. A.; Hahndorf, I.; Illenberger, E.; Sanche, L. *J. Chem. Phys.* **1998**, *108*, 1309.

(9) Desfrançois, C.; Periquet, V.; Bouteiller, Y.; Schermann, J. P. *J. Chem. Phys. A* **1998**, *102*, 1274.

(10) Oyler, N. A.; Adamowicz, L. *J. Phys. Chem.* **1993**, *97*, 11122.

(11) Oyler, N. A.; Adamowicz, L. *Chem. Phys. Lett.* **1994**, *219*, 223. Roerig, G. H.; Oyler, N. A.; Adamowicz, L. *Chem. Phys. Lett.* **1994**, *225*, 265. Roerig, G. H.; Oyler, N. A.; Adamowicz, L. *J. Phys. Chem.* **1995**, *99*, 14285.

(12) Dolgounitcheva, O.; Zakrzewski, V. G.; Ortiz, J. V. *Chem. Phys. Lett.* **1999**, *307*, 220.

(13) Desfrançois, C.; Abdoul-Carime, H.; Schermann, J. P. *J. Chem. Phys.* **1996**, *104*, 7792.

(14) Hendricks, J. H.; Lyapustina, S. A.; de Clercq, H. L.; Bowen, K. H. *J. Chem. Phys.* **1998**, *108*, 8.

(15) Smets, J.; McCarthy, W. J.; Adamowicz, L. *J. Phys. Chem.* **1996**, *100*, 14655.

(16) Smets, J.; Smith, D. M. A.; Elkadi, Y.; Adamowicz, L. *J. Phys. Chem. A* **1997**, *101*, 9152.

(17) Nguyen, M. T.; Chandra, A. K.; Zeegers-Huyskens, T. *J. Chem. Soc., Faraday Trans.* **1998**, *94*, 1277. (b) Chandra, A. K.; Nguyen, M. T.; Zeegers-Huyskens, T. *J. Chem. Phys.* **1998**, *102*, 6010.

(18) Mourik, T. van; Price, S. L.; Clary, D. C. *J. Phys. Chem. A* **1999**, *103*, 1611.

(19) Ortiz, J. V. In *Computational Chemistry: Reviews of Current Trends, Vol. 2*; Leszczynski, J., Ed.; World Scientific: Singapore, 1997; p 1. (b) Ortiz, J. V.; Zakrzewski, V. G.; Dolgounitcheva, O. In *Conceptual Perspectives In Quantum Chemistry, Vol. 3*; Calais, J.-L., Kryachko, E., Eds.; Kluwer: Dordrecht, 1997; p 465. (c) Ortiz, J. V. *Adv. Quantum Chem.* **1999**, *35*, 33 and references therein.

(20) Bartlett, R. J. *Annu. Rev. Phys. Chem.* **1981**, *32*, 359 and references therein.

(21) *GAUSSIAN 98* (Revision A2); Frisch, M. J.; Trucks, G. W.; Schlegel, H. B.; Scuseria, G. E.; Robb, M. A.; Cheeseman, J. R.; Zakrzewski, V. G.; Montgomery, Jr., J. A.; Stratmann, R. E.; Burant, J. C.; Dapprich, S.; Millam, J. M.; Daniels, A. D.; Kudin, K. N.; Strain, M. C.; Farkas, O.; Tomasi, J.; Barone, V.; Cossi, M.; Cammi, R.; Mennucci, B.; Pomelli, C.; Adamo, C.; Clifford, S.; Ochterski, J.; Peterson, G. A.; Ayala, P. Y.; Cui, Q.; Morokuma, K.; Malick, D. K.; Rabuck, A. D.; Raghavachari, K.; Foresman, J. B.; Cioslowski, J.; Ortiz, J. V.; Stefanov, B. B.; Liu, G.; Liashenko, A.; Piskorz, P.; Komaromi, I.; Gomperts, R.; Martin, R. L.; Fox, D. J.; Keith, T.; Al-Laham, M. A.; Peng, C. Y.; Nanayakkara, A.; Gonzalez, C.; Challacombe, M.; Gill, P. M. W.; Johnson, B.; Chen, W.; Wong, M. W.; Andres, J. L.; Head-Gordon, M.; Replogle, E. S.; Pople, J. A. Gaussian, Inc.: Pittsburgh, PA, 1998.

(22) Hehre, W. J.; Ditchfield, R.; Pople, J. A. *J. Chem. Phys.* **1972**, *56*, 2257. Hariharan, P. C.; Pople, J. A. *Theor. Chim. Acta* **1973**, *28*, 213.

(23) Krishnan, R.; Binkley, J. S.; Seeger, R.; Pople, J. A. *J. Chem. Phys.* **1980**, *72*, 650. Petersson, G. A.; Bennett, A.; Tensfeldt, T. G.; Al-Laham, M. A.; Shirley, W. A.; Mantzaris, J. *J. Chem. Phys.* **1988**, *89*, 2193; Petersson, G. A.; Al-Laham, M. A. *J. Chem. Phys.* **1991**, *94*, 6081. Clark, T.; Chandrasekhar, J.; Spitznagel, G. W.; Schleyer, P. von R. *J. Comput. Chem.* **1983**, *4*, 294.

(24) Schlegel, H. B. *J. Chem. Phys.* **1986**, *84*, 4530.

(25) Frisch, M. J.; Pople, J. A.; Binkley, J. S. *J. Chem. Phys.* **1984**, *80*, 3265.

(26) Niessen, W. von; Schirmer, J.; Cederbaum, L. S. *Comput. Phys. Rep.* **1984**, *1*, 57. (b) Zakrzewski, V. G.; Niessen, W. von *J. Comput. Chem.* **1993**, *14*, 13. (c) Zakrzewski, V. G.; Ortiz, J. V. *Int. J. Quantum Chem.* **1995**, *53*, 583.

(27) Schaftenaar, G. MOLDEN 3.4; CAOS/CAMM Center, The Netherlands, 1998.

(28) Boys, S. F.; Bernardi, F. *Mol. Phys.* **1970**, *19*, 553.

(29) Leszczynski, J. *J. Phys. Chem.* **1992**, *96*, 1649.

(30) von Niessen, W., private communication.

(31) Zakrzewski, V. G.; Ortiz, J. V.; Nichols, J. A.; Heryadi, D.; Yeager, D. L.; Golab, J. T. *Int. J. Quantum Chem.* **1996**, *60*, 29.

(32) Sevilla, M. D., private communication.